Biochemical Journal (2018) **475** 3087–3103
https://doi.org/10.1042/BCJ20180247

PORTLAND PRESS

Research Article

An Aβ42 variant that inhibits intra- and extracellular amyloid aggregation and enhances cell viability

Ofek Oren[1,2,3], Victor Banerjee[2,3], Ran Taube[1] and Niv Papo[2,3]

[1]The Shraga Segal Department of Microbiology, Immunology and Genetics, Faculty of Health Sciences, Ben-Gurion University of the Negev, PO Box 653, Beer Sheva 84105, Israel; [2]Department of Biotechnology Engineering, Faculty of Engineering, Ben-Gurion University of the Negev, PO Box 653, Beer Sheva 84105, Israel; [3]The National Institute for Biotechnology in the Negev, PO Box 653, Beer Sheva 84105, Israel

Correspondence: Ran Taube (rantaube@bgu.ac.il) or Niv Papo (papo@bgu.ac.il)

Aggregation and accumulation of the 42-residue amyloid β peptide (Aβ42) in the extracellular matrix and within neuronal cells is considered a major cause of neuronal cell cytotoxicity and death in Alzheimer's disease (AD) patients. Therefore, molecules that bind to Aβ42 and prevent its aggregation are therapeutically promising as AD treatment. Here, we show that a non-self-aggregating Aβ42 variant carrying two surface mutations, F19S and L34P ($Aβ42_{DM}$), inhibits wild-type Aβ42 aggregation and significantly reduces Aβ42-mediated cell cytotoxicity. In addition, $Aβ42_{DM}$ inhibits the uptake and internalization of extracellularly added pre-formed Aβ42 aggregates into cells. This was the case in both neuronal and non-neuronal cells co-expressing Aβ42 and $Aβ42_{DM}$ or following pre-treatment of cells with extracellular soluble forms of the two peptides, even at high Aβ42 to $Aβ42_{DM}$ molar ratios. In cells, $Aβ42_{DM}$ associates with Aβ42, while *in vitro*, the two soluble recombinant peptides exhibit nano-molar binding affinity. Importantly, $Aβ42_{DM}$ potently suppresses Aβ42 amyloid aggregation *in vitro*, as demonstrated by thioflavin T fluorescence and transmission electron microscopy for detecting amyloid fibrils. Overall, we present a new approach for inhibiting Aβ42 fibril formation both within and outside cells. Accordingly, $Aβ42_{DM}$ should be evaluated *in vivo* for potential use as a therapeutic lead for treating AD.

Introduction

Among human neurodegenerative diseases, Alzheimer's disease (AD) is the most common, with nearly 47 million patients worldwide [1]. AD is characterized by a sequestration of amyloid β (Aβ) peptides into fibrillar aggregates that ultimately lead to neuronal cell death and subsequently progressive cognitive dysfunction [2,3]. Aβ peptides that form amyloid fibrils and plaques are processed products of the transmembrane amyloid precursor protein (APP), which is expressed at high levels in the brain and is cleaved into 36–43 residue protein segments by the β- and γ-secretase proteolytic enzymes in neuronal cells [4]. The majority of APP cleavage occurs on the plasma membrane of neuronal cells, with the resulting Aβ peptides being subsequently releasing to the extracellular matrix (ECM) to form plaques. Aβ42-containing extracellular plaques are believed to induce microglia activation, resulting in the release and activation of pre-inflammatory cytokines, such as IL-1β, TNF-α, and IFN-γ, leading to neuro-inflammation [5–7]. Although the majority of the aggregated Aβ fibrils are found in the ECM, emerging evidence indicates that Aβ peptides can also accumulate intracellularly to form fibrillar aggregates. Intracellular accumulation and aggregation of Aβ stems from two sources, namely (i) APP cleavage within cells and (ii) re-uptake of Aβ aggregates from the ECM [8–10]. APP cleavage within cells mainly occurs in the Golgi network, endoplasmic reticulum, and endosomes, as well as on mitochondrial membranes, while Aβ aggregates can be localized with these organelles and

Received: 26 March 2018
Revised: 2 September 2018
Accepted: 7 September 2018

Accepted Manuscript online: 13 September 2018
Version of Record published: 10 October 2018

Biochemical Journal (2018) 475 3087–3103
https://doi.org/10.1042/BCJ20180247

in the cytoplasm [11–13]. Aβ accumulation and aggregation within the mitochondria disrupts the activity of this organelle by diminishing the enzymatic activity of respiratory chain complexes III and IV, resulting in increased reactive oxygen species production [14]. Moreover, intracellular Aβ inhibits and disrupts the ubiquitin-proteasome system and alters calcium and synaptic function [15,16]. Together, these effects eventually lead to disruption of calcium homeostasis, altered proteolysis of essential proteins, and increased nitric oxide levels, and eventually, to apoptosis of neuronal cells [11,13,15,16].

Among the numerous inhibitors that bind Aβ and prevent its aggregation, widely used peptide-based inhibitors are designed based on the Aβ oligomer self-assembly motif KLVFF, a hydrophobic cluster on the Aβ peptide surface [17,18]. However, self-association into spherical assemblies of most of these inhibitors reduces their inhibition efficacies and, therefore, diminishes their potential as therapeutics [19]. As Aβ oligomers form high-ordered amyloid fibrils that are enriched in β-sheet elements, other widely used inhibitors that bind Aβ oligomers are structurally designed to target the β-sheet elements of Aβ [19–22], so as to disrupt protein aggregation. Such peptides, like rGffvlkGr-1,5-diaminopentane (where the lower case letters indicate the D form of an amino acid that was used to reduce proteolytic degradation) [23], HKQLPFFEED (also known as H102) [20], and NAVRWSLMRPF (also known as NF11) [24], present moderate to high efficacy in inhibiting Aβ aggregation *in vitro*. Nonetheless, all these peptide-based inhibitors currently lack clinical outcome due to high toxicity, insufficient inhibition activity, or proteolytic degradation [25–27]. As such, the need for new inhibitors is urgent.

The insufficient inhibitory activities of available peptide inhibitors of Aβ aggregation can be explained by the fact that although both the extracellular and intracellular Aβ aggregation induce toxic effects, no existing inhibitors efficiently inhibit such aggregation at both sites. In addition, most attempts to develop Aβ aggregation inhibitors, such these described above [17–24,26], relied on studies largely performed *in vitro*, mostly addressing extracellular Aβ aggregation and measuring aggregation inhibition *in vitro* [8]. In contrast, only few studies have been conducted in cells, such as a recent study in which the human molecular chaperone DnaJB6 was employed as an inhibitor, targeting Aβ intracellular aggregation. DnaJB6 was, however, unable to inhibit aggregation of extracellular Aβ42 [28].

In this study, we used an Aβ42 variant carrying two mutations, F19S and L34P (designated $Aβ42_{DM}$) and evaluated its efficiency in inhibiting Aβ42 aggregation both *in vitro* and in cells. We further tested the ability of $Aβ42_{DM}$ to rescue cell viability in response to Aβ-mediated toxic effects. $Aβ42_{DM}$ was previously characterized in bacteria as a non-aggregating form of Aβ42 [29,30]. Substitution of the hydrophobic phenylalanine at position 19, part of the central KLVFF hydrophobic cluster in Aβ42, with the polar amino acid serine disrupted Aβ42 self-assembly and perturbed its conformation by altering the steric nature and polarity of the peptide, resulting in reduced aggregation [31,32]. Positions 33–36 in the Aβ sequence are also known to form a hydrophobic region, which is involved in Aβ peptide self-assembly. Previous studies have shown that changing position 34 in Aβ affects peptide conformation and polarity, as well as the ability to self-aggregate [30,33,34]. Moreover, a combination of the F19S and the L34P mutations was previously shown to prevent Aβ self-assembly more efficiently than either single-point mutations introduced separately, disrupting the predominantly β-sheet conformation associated with wild-type Aβ42 [30]. Similar characteristics of Aβ42 variants carrying the F19S and additional mutations were also observed in neuronal cells [35].

To test our hypothesis that $Aβ42_{DM}$ can act as efficient inhibitor of Aβ42 aggregation not only *in vitro* but also in cells, we employed a mammalian cell-based platform in which expression of an Aβ42-GFP fusion protein served as a reporter of Aβ42 aggregation. Our results show that $Aβ42_{DM}$ binds Aβ42, inhibits its aggregation, and reduces Aβ42 cytotoxic effects when co-expressed with Aβ42, or when supplemented externally, in both HEK293T and SH-SY5Y neuroblastoma cells. We also show that $Aβ42_{DM}$ prevents the uptake and internalization of aggregated Aβ42 fibrils into neuronal cells, and thus has the potential to serve as a therapeutic lead in the search for drugs treating AD.

Methods

Cells and transfection

HEK293T cells were purchased from ATCC (Manassas, VA). SH-SY5Y neuroblastoma cell line was a generous gift from Prof. Varda Shoshan-Barmatz (BGU). HEK293T and SH-SY5Y cells were grown at 37°C and 5% CO_2 in Dulbecco's modified Eagle medium (DMEM) supplemented with 10% tetracycline-free fetal bovine serum (FBS), L-glutamine (2 mM), and penicillin (100 units/ml)/streptomycin (0.1 mg/ml) (Gibco, Israel). Transfection

was performed using Lipofectamine 2000 transfection reagent (Thermo-Fisher, Waltham, MA) for HEK293T cells or Turbofect (Thermo-Fisher) for SH-SY5Y cells, according to the protocol of the manufacturer. When co-transfections were performed, empty plasmids were transfected as controls.

Plasmids

The Aβ42-GFP gene where Aβ42 is fused to GFP (a generous gift from Michael Hecht, Princeton University) was cloned into the pHAGE lentivector, in which transcription is under the control of the CMV promoter. The pHAGE vector also expresses a puromycin resistance selection marker that follows an internal ribosome entry site (IRES) sequence. Plasmid pHAGE $A\beta42_{F19S,L34P}$-GFP ($A\beta42_{DM}$-GFP) was generated by two consecutive rounds of directed mutagenesis of Aβ42 at positions 19 and 34. We also generated pHAGE HA-$A\beta42_{DM}$-IRES-BFP lentivector, and plasmids pCDNA3.1-HA-$A\beta42_{DM,}$ pCDNA3.1-HA-$A\beta42_{DM}$-BFP, and pCDNA3.1-HA-$A\beta42_{DM}$-Fc. The $A\beta42_{DM}$ gene was amplified by PCR and fused to DNA encoding an N-terminal human influenza hemagglutinin (HA)-tag, and later cloned into the pHAGE2 or pCDNA3.1 expression vectors with one of the indicated markers. All plasmids are shown in Supplementary Figure S1.

Production of pseudo-typed lentivirus

HEK293T cells were transfected with the gene of interest using the packaging HIV expression plasmids pGag-Pol, pRT, pTat, and pREv and the envelope VSV-G protein by the calcium phosphate method. Cell supernatant containing the virus was collected 48 h post-transfection, cleared through a 0.45 μm filter, and further concentrated by centrifugation (2000 rpm, 10 min) to obtain a high titer viral stock that was then aliquoted and stored at −80°C. To determine viral titer, 5×10^4 HEK293T cells were plated on 24-well plates and infected with serial dilutions of the indicated VSV-G pseudo-typed virus CMV-GFP. Cells were analyzed for GFP expression by FACS.

Generation of stable cell lines

5×10^4 HEK293T and SH-SY5Y cells were seeded in 24-well plates and transduced with lentivirus expressing the relevant genes at 0.75 multiplicity of infection levels. After 72 h following transduction, the cells were subjected to 1.5 μg/ml puromycin selection and/or sorted for GFP and/or BFP expression (when $A\beta42_{DM}$ IRES-BFP was used). The following stable cell lines were generated:

(i) HEK293T Aβ42-GFP (HEK- Aβ42-GFP).
(ii) HEK293T $A\beta42_{DM}$ (HEK-$A\beta42_{DM}$).
(iii) HEK293T Aβ42-GFP and $A\beta42_{DM}$ with low expression (HEK-Aβ42-GFP-$A\beta42_{DM}$L).
(iv) HEK293T Aβ42-GFP and $A\beta42_{DM}$ with high expression (HEK- Aβ42-GFP-$A\beta42_{DM}$H).
(v) SH-SY5Y Aβ42-GFP (SH-Aβ42-GFP); and (vi) SH-SY5Y $A\beta42_{DM}$-GFP (SH-$A\beta42_{DM}$-GFP).

Flow cytometry and cell sorting

For analysis of Aβ42-GFP, $A\beta42_{DM}$-GFP or $A\beta42_{DM}$-IRES-BFP expression in HEK293T or SH-SY5Y cells, cells were harvested, re-suspended with phosphate-buffered saline (PBS) and analyzed by a Beckman Gallios FACS (Faculty of Health Sciences, BGU). For sorting of HEK293T or SH-SY5Y cells stably expressing Aβ42-GFP, $A\beta42_{DM}$-GFP, $A\beta42_{DM}$-IRES-BFP or both Aβ42-GFP and $A\beta42_{DM}$-IRES-BFP, cells were harvested and re-suspended with PBS supplemented with 10% FBS. Cells were analyzed for GFP or BFP expression and sorted using the BD Aria FACS (Ilse Katz Institute for Nanoscale Science & Technology, BGU). HEK293T cells stably expressing both Aβ42-GFP and $A\beta42_{DM}$-IRES-BFP were re-sorted to establish cell populations showing low (L) or high (H) $A\beta42_{DM}$-IRES-BFP expression and similar Aβ42-GFP expression.

Recombinant peptides

Aβ 1-42 peptide and Aβ 1-42-Hylight 488 labeled peptides were purchased from Anaspec (Fremont, CA). Aβ 1-42 F19S, L34P ($A\beta42_{DM}$) peptide was synthesized and purchased from GL-Biochem (Shanghai, China).

Biochemical Journal (2018) 475 3087–3103
https://doi.org/10.1042/BCJ20180247

Aβ seeds preparation

Aβ42 (40 μM) in the presence or absence of $Aβ42_{DM}$ at 1:65 molar ratio ($Aβ42_{DM}$:Aβ42) was incubated in 500 μl of 20 mM sodium phosphate buffer, pH 7.4, 0.15 M NaCl at 37°C with orbital shaking for 72 h, followed by centrifugation at 20 K G for 1 h. Pellet was dissolved in 50 μl of PBS and aliquoted.

Confocal microscopy

HEK293T or SH-SY5Y cells were grown on 1 cm micro-slides and transfected using Lipofectamine or turbofect, respectively, with a total of 0.5 μg DNA, as indicated in Table S1. For monitoring Aβ42-488 internalization, SH-SY5Y cells were incubated with 500 nM extracellular pre-formed Aβ42-488 labeled peptide fibrils in the presence or absence of 7.75 nM of the $Aβ42_{DM}$ peptide. Forty-eight hours post-transfection of Aβ42, or 18 h after adding the soluble Aβ42-488 peptide, images of live cells were taken using an Olympus FV1000 confocal microscope with a long-working distance ×60/1.35 numerical aperture oiled-immersion objective [The National Institute for Biotechnology in the Negev (NIBN), BGU]. Nuclear staining was conducted using Hoechst dye (Thermo-Fisher, Israel), diluted 1/2000 in PBS, while membrane staining was performed with FM 4-64 dye (10 μg/ml final concentration; Thermo-Fisher).

Intracellular protein aggregation quantification

Confocal images of HEK293T cells overexpressing Aβ42-GFP, $Aβ42_{DM}$ or a combination of both proteins at different expression levels were analyzed as above. Images of the number of cells containing Aβ42-GFP aggregates from 3 independent experiments were analyzed using the ImageJ software. Values were normalized to cells expressing only Aβ42-GFP. Quantitative analysis ($n = 3$) was performed by unpaired Student's *t*-test. **, $P < 0.05$; ***, $P < 0.005$.

Quantification of Aβ42 internalization

SH-SY5Y cells were incubated with 500 nM of Aβ42-488 in the absence or presence of 7.75 nM $Aβ42_{DM}$. Images were taken 18 h post-incubation with the Operetta high-content imaging system with ×40 magnification (NIBN, BGU). Nuclear and membrane staining were performed as described above. Images were analyzed using the Columbus software and levels of fluorescence intensity at 488 nm in the cytosol were determined. All measurements were done in triplicate and different regions of each well were imaged. Quantitative analysis ($n = 3$) was performed by unpaired Student's *t*-test. **, $P < 0.05$; ***, $P < 0.005$.

Immunoprecipitation and western blot analysis

4×10^6 naïve or transformed HEK293T or SH-SY5Y cells were seeded in 10 cm plates. HEK293T cells were transfected to express Aβ42-GFP, $Aβ42_{DM}$-Fc, or a combination of both using a total of 15 μg DNA. The cells were harvested and lysed with IP (immunoprecipitation) buffer [20 mM Tris–HCl, pH 7.6, 200 mM NaCl, 0.72 mM EDTA, 10% glycerol, 7 mM DTT, and protease inhibitor (PI) cocktail (Sigma–Aldrich, Israel) which was added fresh before use at a ratio of 1:200, and 0.15% Triton X-100]. The solubilized cell fraction was incubated with pre-blocked magnetic protein G Dynabeads (Invitrogen, Carlsbad, CA) according to the manufacturer's instructions. The beads were magnetically isolated and washed three times with PBS, and suspended with sample buffer (6.25 mM Tris–HCl, pH 6.8, 10% glycerol, bromophenol blue, 2% SDS, 5% β-mercaptoethanol). The samples were heated for 5 min at 95°C and separated by 15% SDS–PAGE and subjected to WB (western blot). Proteins in the gel were transferred to a nitrocellulose membrane at 110 V for 45 min, which was probed with anti-GFP antibodies (Abcam, Cambridge, MA) diluted 1/1000 in PBS to detect Aβ42-GFP fusion protein, anti-Fc horseradish peroxidase (HRP)-conjugated antibodies (Jackson, West Grove, PA) diluted 1/1000 in PBS to detect $Aβ42_{DM}$-Fc, or anti-β tubulin antibodies (Abcam) diluted 1/500 in PBS. HRP-conjugated anti-mouse and anti-rabbit antibodies (Jackson) were used as secondary antibodies. Antibody binding was revealed using an enhanced chemiluminescence kit (Biological Industries).

To monitor the level of transiently expressed Aβ42-GFP or $Aβ42_{DM}$-GFP, cells were grown on 10 cm plates (10^7 cells per plate), harvested, and washed with PBS. Cell pellets were then suspended with RIPA buffer (25 mM HEPES-NaOH, 150 mM KCl, 1 mM EDTA, 1% Triton X-100, 0.1% NP-40, pH7.4, fresh (PIs cocktail (1:200; Sigma–Aldrich). Protein concentrations were determined by Bradford assay (Bio-Rad, Hercules, CA) and 100 μg of total cell lysates was supplemented with sample buffer before 15% SDS–PAGE. Following

Biochemical Journal (2018) 475 3087–3103
https://doi.org/10.1042/BCJ20180247

transfer to nitrocellulose membranes, the separated proteins were probed with anti-Aβ42 IgG (Sigma–Aldrich) or anti-β tubulin antibodies (Abcam) as described above.

To monitor Aβ42 fibrils and aggregate formation in the absence or presence of $Aβ42_{DM}$, 360 ng of Aβ42 with or without 6 or 0.75 ng of $Aβ42_{DM}$, or 6 ng of $Aβ42_{DM}$ alone was supplemented with sample buffer, boiled, and separated on a 4–15% gradient SDS–PAGE gel (Bio-Rad). WB was performed using anti-Aβ42 antibodies (Sigma–Aldrich) as described above.

Dot blot experiment

Aβ42 samples (5 µl) incubated for 18 h were applied to nitrocellulose membranes. The membrane was blocked for 1 h with 5% non-fat milk in PBS followed by incubation with A11 antibodies (Thermo-Fisher) at 1:1000 dilution in PBS containing 5% non-fat milk. HRP-conjugated anti-rabbit antibodies (Jackson) were used as secondary antibodies. Antibody binding was revealed using an enhanced chemiluminescence kit (Biological Industries).

XTT cell viability assay

The viability of HEK293T and SH-SY5Y stable cell lines (described above) or SH-SY5Y cells incubated with Aβ42 fibrils in the absence or presence of different concentrations of $Aβ42_{DM}$ (3.5–32 nM) was assessed using an XTT-based kit (Biological Industries) according to the manufacturer's protocol. Briefly, 10^4 cells per well were seeded in a 96-well plate. Twenty-four hours after treatment, cell viability was determined. Naïve HEK2393T or SH-SY5Y cells served as controls for these experiments. Data for each assay were normalized relative to the control and are presented as percentage of control. Experiments were performed in triplicate. Quantitative analysis ($n = 3$) was performed by unpaired Student's t-test. ** $P < 0.05$; *** $P < 0.005$.

Thioflavin T aggregation assay

Assays were performed, as described previously [36]. Briefly, Aβ42 (4 µM) with or without $Aβ42_{DM}$ was incubated in 200 µl of 20 mM sodium phosphate buffer, pH 7.4, 0.15 M NaCl to which 10 µM of ThT (thioflavin T) (Sigma–Aldrich, Israel) was added. Reactions were performed in a black 96-well plate at 37°C shaken at 300 rpm in a Tecan Infinite M1000 plate reader with fluorescence excitation and emission wavelengths set at 440 and 485 nm, respectively. ThT fluorescence was measured at 10 min intervals. Each experiment was performed in triplicate.

Monitoring Aβ42 oligomerization by light scattering

Aβ42 peptides (4 µM) were incubated in 200 µl of 20 mM Na^+/phosphate buffer, pH 7.4, 0.15 M NaCl, in a black 96-well plate (transparent bottom) at 37°C with 250 rpm continuous orbital shaking using the Infinite M1000 (Männedorf, Switzerland; Cytometry and Proteomics unit, NIBN, BGU) plate reader in the presence or absence of $Aβ42_{DM}$. Light scattering was monitored at 400 nm over 18 h of incubation.

Circular dichroism

CD (circular dichroism) spectra were recorded on a Jasco J715 spectropolarimeter over a range of 190–260 nm using a quartz cuvette with a path length of 1 mm, a scanning speed of 50 nm/min, and a data interval of 1 nm, at 25°C. Twenty micromolars Aβ42 samples in the absence or presence of $Aβ42_{DM}$ (62 nM) were incubated for 18 h in 20 mM Na^+/phosphate buffer, pH 7.4, 0.15 M NaCl. Each sample was scanned four times at time zero and 18 h post-incubation. Scans were averaged to obtain smooth data and background corrected with respect to protein-free buffer.

TEM sample preparation

Samples for TEM imaging were prepared as described [37]. Briefly, after 70 h of incubation, 2.5 µl aliquots of the samples (see ThT assay samples) were deposited on carbon-coated copper 300 mesh grids. After 1 min, excess liquid was carefully blotted with filter paper, and the grid was held at ambient temperature for another minute. Uranyl acetate (2%, 5 µl) was added for 1 min, after which time any excess solution was carefully removed with filter paper. Imaging was performed using a Tecnai G2 12 BioTWIN (FEI) (Ilse Katz Institute for Nanoscale Science & Technology, BGU) TEM with an acceleration voltage of 120 kV. Variable magnifications were used for visualization, depending on the size of the aggregates.

Biochemical Journal (2018) 475 3087–3103
https://doi.org/10.1042/BCJ20180247

Surface plasmon resonance spectroscopy

The constants for the binding of $A\beta42_{DM}$ to Aβ42 were determined by SPR (surface plasmon resonance) spectroscopy on a ProteOn XPR36 (Bio-Rad) [38], as follows. $A\beta42_{DM}$ or Aβ42 was immobilized on the surface of the chip using the amine coupling reagents, sulfo-NHS (0.1 M *N*-hydroxysuccinimide) and EDC [0.4 M 1-ethyl-3-(3-dimethylaminopropyl)-carbodiimide] (Bio-Rad). $A\beta42_{DM}$ or Aβ42 (20 μg) was covalently immobilized on the chip in 10 mM sodium acetate buffer, pH 4.0, to obtain 1663 response unit (RU). Bovine serum albumin (BSA; 3 μg, 3432 RU) was immobilized on the chip as a negative control, using a different flow channel. Unbound esters were deactivated with 1 M ethanolamine HCl at pH 8.5. Before each binding assay, the temperature was set at 25°C. Soluble human Aβ42 or $A\beta42_{DM}$ (the analyte) was then allowed to flow over surface-bound $A\beta42_{DM}$/Aβ42 at concentrations of 0, 0.125, 0.25, 0.5, 1, and 2 μM and a flow rate of 50 μl/min. While the analyte was flowing over the surface (for 16 min), interactions between $A\beta42_{DM}$ and Aβ42 were determined. Dissociation of the proteins was next examined by allowing PBST (PBS, 50 mM NaCl, 0.05% Tween 20) to flow over the surface for 28 min at 50 μl/min. After each run, a regeneration step was performed with 50 mM NaOH at a flow rate of 100 μl/min. For each protein complex, a sensorgram was generated from the RUs measured over the course of the protein–protein interaction minus the values from the BSA background channel. The k_{on} and k_{off} were determined by fitting the data points using a 1:1 Langmuir kinetic model [38]. The fitted data were considered statistically valid as the χ^2 value was less than the 10% of the Rmax in the fitted graphs [38].

Results

$A\beta42_{DM}$ suppresses Aβ42 aggregation in cells

In the present study, we initially traced Aβ42 intracellular expression and aggregation in human cells. Previous studies showed that an Aβ42-GFP fusion protein could serve as a reporter for protein misfolding and aggregation in bacteria, since Aβ42 aggregates more rapidly than the GFP protein folds, causing GFP to misfold and hence lose its fluorescence [29,30]. In contrast, the Aβ42 variant mutant $A\beta42_{F19S,L34P}$ ($A\beta42_{DM}$) does not aggregate. Indeed, when fused to GFP, proper folding and preserved GFP fluorescence ensue. To verify that expression levels and aggregation patterns of Aβ42-GFP and $A\beta42_{DM}$-GFP were similarly maintained in human cells, we expressed Aβ42-GFP or $A\beta42_{DM}$-GFP in HEK293T cells and followed GFP fluorescence as a marker Aβ42 aggregation by flow cytometry and confocal microscopy (Figure 1). Our results show that in human cells, Aβ42-GFP displayed low intensity fluorescence, indicating that the GFP moiety was not properly folded. This was accompanied by visible intracellular protein aggregation, probably reflecting Aβ42-GFP inclusion bodies found in the cytoplasm of the HEK cells (Figure 1A,B). In contrast, $A\beta42_{DM}$-GFP exhibited 10-fold higher intensity fluorescence than Aβ42-GFP, implying correct folding. Moreover, $A\beta42_{DM}$-GFP displayed a diffuse and non-aggregated pattern of expression (Figure 1A,B). These findings confirm the earlier work performed in bacteria and demonstrate the distinctive folding patterns of Aβ42 and $A\beta42_{DM}$ when expressed in mammalian cells [28,39,40].

To ensure that the differences in GFP fluorescence levels and Aβ42 aggregation (i.e. the amount of inclusions bodies) displayed by Aβ42 or $A\beta42_{DM}$ are not a result of different expression levels of the two proteins in HEK293T, we tested the expression of both proteins by WB analysis. Surprisingly, $A\beta42_{DM}$ was expressed 2.8-fold better than Aβ42 (Figure 1C). Comparing the 2.8-fold difference in the expression of $A\beta42_{DM}$ over that of Aβ42 to the 10-fold difference in fluorescence suggests that the increased fluorescence of $A\beta42_{DM}$ was not only due to augmented expression of this variant. To validate that the differences in aggregation patterns and fluorescence/expression levels between Aβ42-GFP and $A\beta42_{DM}$-GFP in HEK293T cells were also the case in neuronal cells, we expressed Aβ42-GFP or $A\beta42_{DM}$-GFP in the SH-SY5Y neuroblastoma cell line, a well-established cell model for neuronal disorders (Supplementary Figure S2). Our results showed that, similar to what was seen in HEK293T cells, Aβ42-GFP expression resulted in low levels of diffused fluorescence in the cytoplasm, which was accompanied by protein aggregates (Supplementary Figure S2B). At the same time, $A\beta42_{DM}$-GFP expression led to high levels of diffused fluorescence and no inclusions bodies (Supplementary Figure S2D).

To monitor the ability of $A\beta42_{DM}$ to inhibit Aβ42-GFP aggregation, we transiently co-expressed the two proteins in HEK293T cells and monitored Aβ42-GFP aggregation using confocal microscopy (Figure 1D,E). Our results showed that when co-expressed, $A\beta42_{DM}$ suppressed Aβ42-GFP aggregation up to 90%, relative to what was seen in cells that expressed Aβ42-GFP alone. Significantly, this reduction was $A\beta42_{DM}$-dose dependent, as

Biochemical Journal (2018) **475** 3087–3103
https://doi.org/10.1042/BCJ20180247

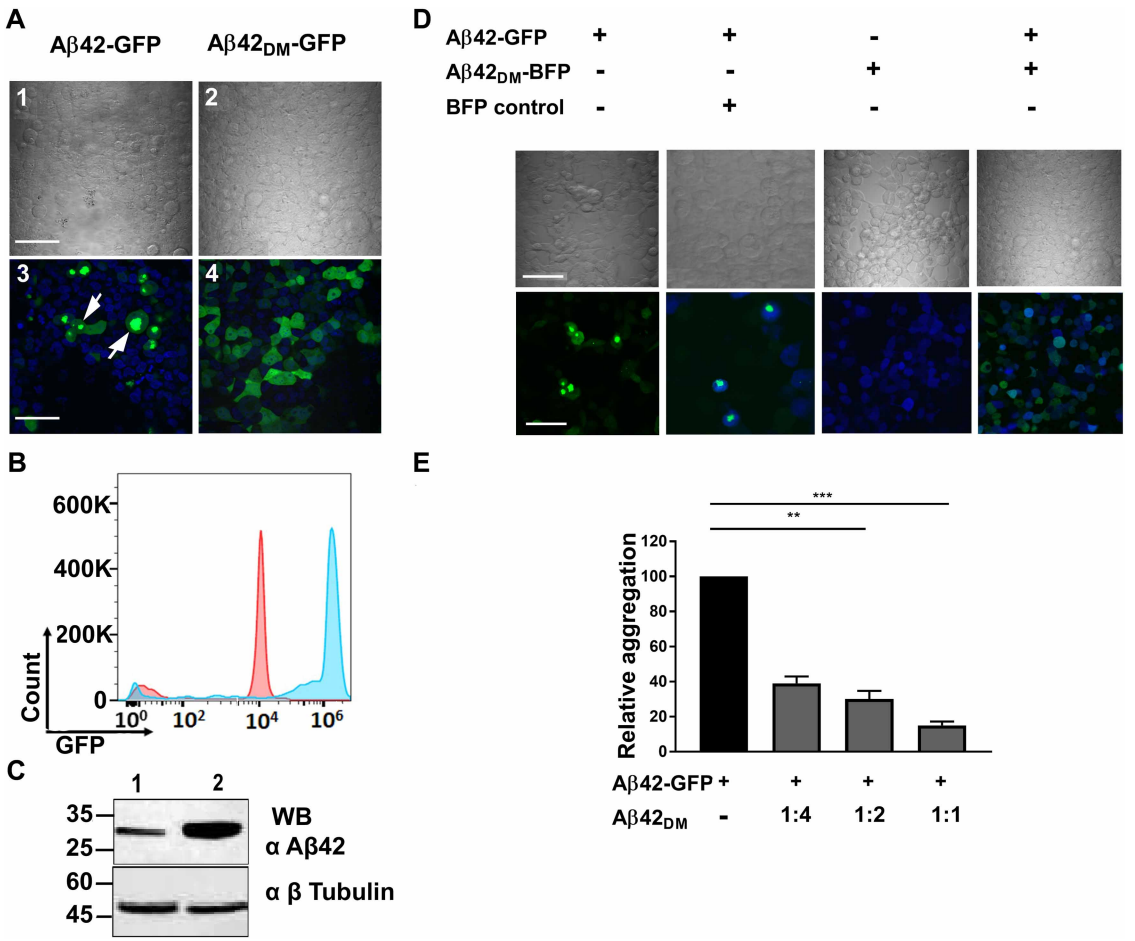

Figure 1. Aβ42$_{DM}$ prevents Aβ42 aggregation in cells.

(**A**) Aβ42 but not Aβ42$_{DM}$ aggregates in cells. Live confocal microscopy imaging of HEK293T cells transiently expressing either Aβ42-GFP (panels 1 and 3) or Aβ42$_{DM}$-GFP (2 and 4). White arrows indicate Aβ42 aggregates. Imaging was performed using an Olympus confocal microscope. Hoechst stain was used for nuclear staining. Scale bars indicate 150 μm. Panels 1 and 2 show bright field and panels 3 and 4 fluorescence. (**B**) FACS analysis of Aβ42-GFP (red) or Aβ42$_{DM}$-GFP (blue) GFP intensity. Fluorescence geometric means are 5189 for Aβ42-GFP and 50808 for Aβ42$_{DM}$-GFP. (**C**) WB analysis of HEK293T cell lysate transiently expressing Aβ42-GFP (lane 1) or Aβ42$_{DM}$-GFP (lane 2). Cells were lysed with RIPA buffer and analyzed by 15% SDS–PAGE followed by WB with anti-Aβ42 antibody. β-tubulin served as an internal control for whole cell extract protein amounts, as revealed by WB with anti-β-tubulin antibodies. (**D**) Aβ42$_{DM}$ inhibits Aβ42 aggregation in cells. Live imaging confocal microscopy of HEK293T cells transiently expressing the indicated proteins. Imaging was performed using Olympus confocal microscope. Scale bars indicate 150 μm. Upper panels show bright field and lower panel fluorescence. (**E**) Quantification of intracellular aggregation in cells expressing Aβ42-GFP or co-expressing Aβ42-GFP and Aβ42$_{DM}$ in a dose-dependent manner (Supplementary Figure S3). Confocal images of HEK293T cells transiently expressing either Aβ42-GFP (black) or Aβ42-GFP and Aβ42$_{DM}$ at different expression ratios (gray) of 1:4, 1:2, or 1:1 (Aβ42$_{DM}$:Aβ42-GFP). ImageJ software was used to count intracellular aggregates in each image. Data from each treatment were normalized to the level of Aβ42-GFP aggregation. Quantitative analysis ($n = 3$) was performed by unpaired Student's *t*-test. **, $P < 0.05$; ***, $P < 0.005$. Error bars indicate the standard error of independent experiments performed in triplicate.

increasing the amount of Aβ42$_{DM}$ led to a reduction in the numbers of Aβ42-GFP inclusion bodies seen. To ensure that the inhibitory effect of Aβ42$_{DM}$ was not due to interactions between Aβ42$_{DM}$ and GFP, we performed an IP experiment with Aβ42$_{DM}$ and GFP in HEK293T cells; no association was detected

Biochemical Journal (2018) 475 3087–3103
https://doi.org/10.1042/BCJ20180247

(Supplementary Figure S4). These findings highlight the ability of $A\beta42_{DM}$ to inhibit Aβ42 aggregation in human cells.

$A\beta42_{DM}$ associates with Aβ42

Having demonstrated that $A\beta42_{DM}$ effectively inhibits Aβ42 intracellular aggregation in HEK293T cells, we next sought to elucidate the mechanism involved. To this end, we monitored the interaction between $A\beta42_{DM}$ and Aβ42 in cells. Aβ42-GFP and $A\beta42_{DM}$-Fc-fusion proteins were co-expressed in HEK293T cells, followed by co-IP with protein G beads and followed by WB analysis. Our results showed that $A\beta42_{DM}$ is associated with Aβ42 in cells (Figure 2A).

To confirm direct binding between Aβ42 and $A\beta42_{DM}$ *in vitro* and to further illuminate the effect of $A\beta42_{DM}$ on Aβ42 aggregation kinetics, we used $A\beta42_{DM}$ and Aβ42 peptides and monitored their direct binding by SPR spectroscopy. The parameters of binding were computed by fitting the SPR sensorgrams using a Langmuir 1:1 binding model (Figure 2B,C). Our results showed that when immobilized to the chip, $A\beta42_{DM}$ binds Aβ42 with k_{on} and k_{off} rates of 300 M^{-1} s^{-1} and 1.6 × 10^{-4} s^{-1}, respectively, with the K_D for the interaction being 520 nm (Figure 2B). However, when Aβ42 is immobilized, no binding was detected (Figure 2C). The fusion of Aβ42 with the chip forced the protein to persist as a monomer, whereas in solution, the protein started to undergo oligomerization. Consequently, these results imply that $A\beta42_{DM}$ binds to oligomeric but not monomeric Aβ42.

$A\beta42_{DM}$ suppresses Aβ42 aggregation and fibril formation *in vitro*

To monitor the effect of $A\beta42_{DM}$ on Aβ42 aggregation kinetics *in vitro*, we co-incubated the two peptides at different molar ratios and followed the progress of Aβ42 amyloid aggregation by staining with ThT, an amyloid-specific staining dye (Figure 3A). Our results show that Aβ42 exhibits a typical aggregation pattern with a ∼2 h lag phase (Supplementary Figure S5A) and that low concentrations of purified $A\beta42_{DM}$ (15 nM) were sufficient to significantly suppress Aβ42 aggregation (at 4 μM) (Figure 3A). Importantly, $A\beta42_{DM}$ at 7.8–62 nM did not self-aggregate or form fibrils, as shown by ThT staining (Supplementary Figure S5B). In addition, TEM images revealed the presence of fibrillar aggregates of untreated Aβ42 after 60 h of incubation. This experiment further showed that adding $A\beta42_{DM}$ and Aβ42 at molar ratios of ∼1:266 or ∼1:65 ($A\beta42_{DM}$:Aβ42) significantly reduced Aβ42 fibrillation (Figure 3B). This was also shown by WB analysis (Figure 3C), demonstrating significant inhibition of fibril formation in the presence of $A\beta42_{DM}$ at a 1:65 ($A\beta42_{DM}$:Aβ42) molar ratio. Interestingly, adding $A\beta42_{DM}$ after 24 h of Aβ42 aggregation did not affect its further aggregation, suggesting that $A\beta42_{DM}$ does not interact with high molecular-weight oligomers (probably pre-fibrils) that appeared at this time point (Supplementary Figure S6).

Aggregated Aβ42 seeded with monomeric Aβ42 is known to induce and increase the aggregation of monomeric Aβ42 [41]. To further evaluate the ability of $A\beta42_{DM}$ to suppress Aβ42 aggregation, we examined its inhibitory activity by measuring the progression of Aβ42 amyloid aggregation by staining with ThT upon addition of aggregated Aβ42 seeds (Figure 4A). Our results show that the lag phase of Aβ42 was decreased and that aggregation was increased upon the addition of Aβ42 seeds, whereas $A\beta42_{DM}$ was not recruited to aggregate by the seeds. Moreover, $A\beta42_{DM}$ significantly reduced lag phase shortening and the aggregation-inducing effect of the seeds on Aβ42. Importantly, seeds generated from a mixture of Aβ42 and $A\beta42_{DM}$ and reacted with Aβ42 did not increase Aβ42 aggregation and exhibited a strong inhibitory effect (Figure 4B), in terms of both aggregation suppression and lag phase extension, reinforcing $A\beta42_{DM}$ as an efficient inhibitor of Aβ42 aggregation.

$A\beta42_{DM}$ modulates the Aβ42 aggregation pathway

To better understand $A\beta42_{DM}$ mechanism of activity in both cell model and *in vitro*, we investigated whether $A\beta42_{DM}$ prevents Aβ42 self-assembly or otherwise allows Aβ42 oligomerization. We showed that $A\beta42_{DM}$ did not prevent Aβ42 oligomerization in the presence of $A\beta42_{DM}$ at a 1:65 molar ratio ($A\beta42_{DM}$:Aβ42), as shown by light scattering (Figure 5A). Nevertheless, oligomers formed by Aβ42 were recognized by the A11 antibody (Figure 5B), which recognizes toxic 'on-pathway' Aβ oligomers [42,43]. However, in the presence of $A\beta42_{DM}$, the recognition signal was reduced to 83%. These results imply that $A\beta42_{DM}$ did not prevent Aβ42 oligomerization but significantly modulated the aggregation pathway of Aβ42, leading to the formation of 'off-pathway' oligomers. This was also reinforced by CD analysis, showing that while being predominantly unstructured at $t = 0$, the oligomers that formed upon treatment with $A\beta42_{DM}$ for 18 h had less beta sheet content than did untreated

Biochemical Journal (2018) **475** 3087–3103
https://doi.org/10.1042/BCJ20180247

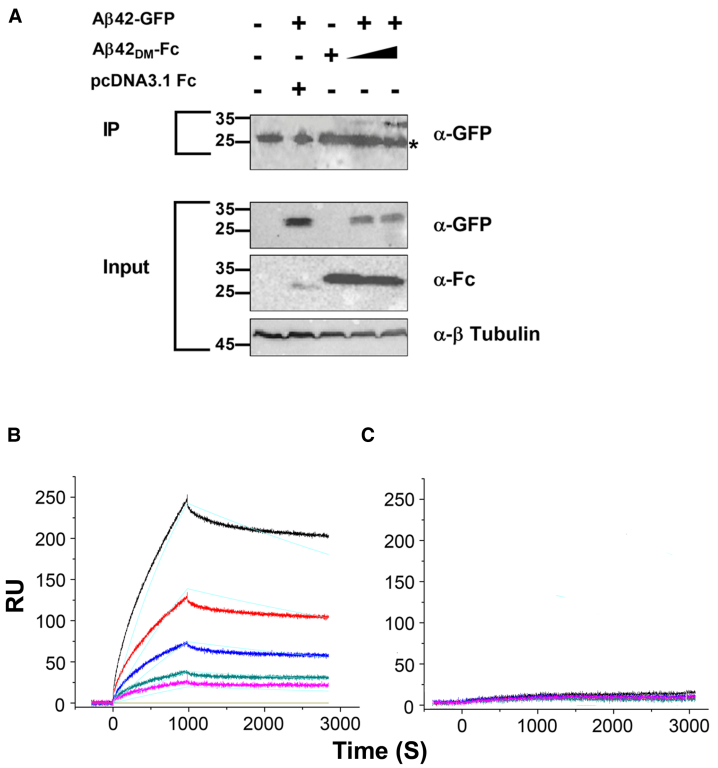

Figure 2. Interaction between Aβ42$_{DM}$ and Aβ42.

(**A**) HEK293T cells transiently expressing Aβ42-GFP, Aβ42$_{DM}$-Fc, or both at different ratios, were lysed and subjected to IP with protein G conjugated to magnetic beads followed by western blotting with anti-GFP antibodies. pCDNA 3.1-Fc empty plasmid was used as a control for Fc expression. The asterisk (*) indicates IgG. (**B** and **C**) Dose–response SPR sensorgrams illustrating binding between Aβ42$_{DM}$ and Aβ42 at different concentrations (grey, magenta, green, blue, red, and black represent 0, 0.125, 0.25, 0.5, 1, and 2 μM of Aβ42, respectively). Either Aβ42$_{DM}$ (**B**) or Aβ42 (**C**) was fused to the chip, while the other peptide served as the analyte. Data points were fitted using a 1:1 Langmuir model, with cyan-colored lines representing the fitted lines.

Aβ42 (lower value of Aβ42 at 216 nm, when compared with treated Aβ42; Supplementary Figure S7). Considering those results and those depicted in Figure 4 showing that Aβ42 aggregates formed in the presence of Aβ42$_{DM}$ behave differently than do Aβ42 aggregates, it is probable that Aβ42$_{DM}$ modulates the Aβ42 aggregation pathway into less-toxic off-pathway oligomers.

Aβ42-induced cell toxicity is suppressed by treatment with intra- and extracellular Aβ42$_{DM}$

Aβ42 intracellular aggregation is considered a pivotal step in inducing neuronal cell death [9]. As our results showed that Aβ42$_{DM}$ inhibits Aβ42-GFP intracellular aggregation in HEK293T cells (Figure 1), we further tested whether Aβ42$_{DM}$ can also protect these cells from intracellular Aβ42-induced toxicity. To do so, we compared the viability of cells expressing Aβ42 to that of cells expressing supposedly non-toxic Aβ42$_{DM}$, or to that of cells expressing both proteins, when naïve HEK293T cells served as control. Aβ42-GFP and Aβ42$_{DM}$-IRES BFP were stably expressed in cells respectively designated as HEK-Aβ42-GFP and HEK-Aβ42$_{DM}$ (Figure 6A). Similarly, stable expression of Aβ42-GFP and Aβ42$_{DM}$-GFP was established in the SH-SY5Y neuroblastoma cell line (Figure 4C,D). In addition, we also generated cells expressing both proteins (designated as HEK-Aβ42-GFP-Aβ42$_{DM}$). Two cell populations that equally expressed Aβ42-GFP but differentially expressed Aβ42$_{DM}$-IRES-BFP were FACS-sorted on the basis of their Aβ42$_{DM}$-IRES-BFP expression levels. The two sorted populations correspond to cells expressed either low (HEK-Aβ42-GFP-Aβ42$_{DM}$L) or high (HEK-Aβ42-GFP-Aβ42$_{DM}$H) Aβ42$_{DM}$ levels (Supplementary Figure S8A–E), the latter expressing Aβ42$_{DM}$ ∼2.5-fold over the level of the low expression population. We then followed Aβ42-GFP-induced cell toxicity by

Biochemical Journal (2018) **475** 3087–3103
https://doi.org/10.1042/BCJ20180247

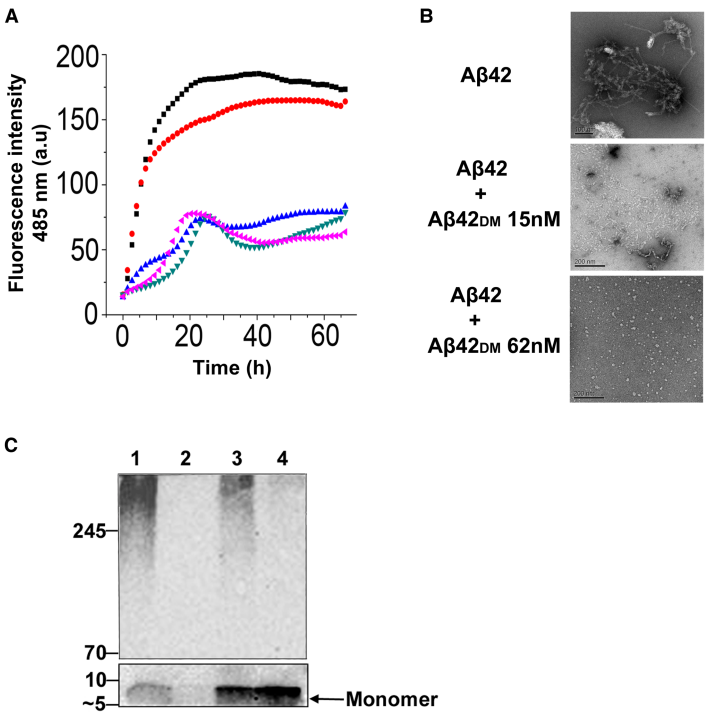

Figure 3. Aggregation kinetics and morphology of Aβ42 aggregates in the presence or absence of $A\beta42_{DM}$.

(**A**) ThT fluorescence was monitored upon co-incubation of Aβ42 (4 μM) with $A\beta42_{DM}$ at different concentrations (black, red, blue, pink, and green represent 0, 7.8, 15.5, 31, and 62 nM, respectively) at 37°C with continuous shaking. (**B**) TEM images of Aβ42 (4 μM) aggregates (upper panel) or Aβ42 co-incubated with $A\beta42_{DM}$ at different concentrations (15 nM, middle panel, and 62 nM, lower panel) after 65 h of incubation. (**C**) WB analysis of 4 μM Aβ42 fibrils in the absence (lane 1) or presence of 7 nM (lane 3) or 62 nM (lane 4) of $A\beta42_{DM}$. 62 nM of $A\beta42_{DM}$ alone (lane 2) served as control.

the XTT cell viability assay. In agreement with the known toxic effects of Aβ42, our results showed that HEK-Aβ42-GFP cells were ∼30% less viable, relative to naïve HEK293T cells or to HEK-$A\beta42_{DM}$ cells (Figure 6A). Moreover, as the toxic effect of Aβ42 is known to cause neuronal cell death, we also examined the toxicity of stable Aβ42-GFP expression by the SH-SY5Y neuroblastoma cell line and noted a toxic effect similar

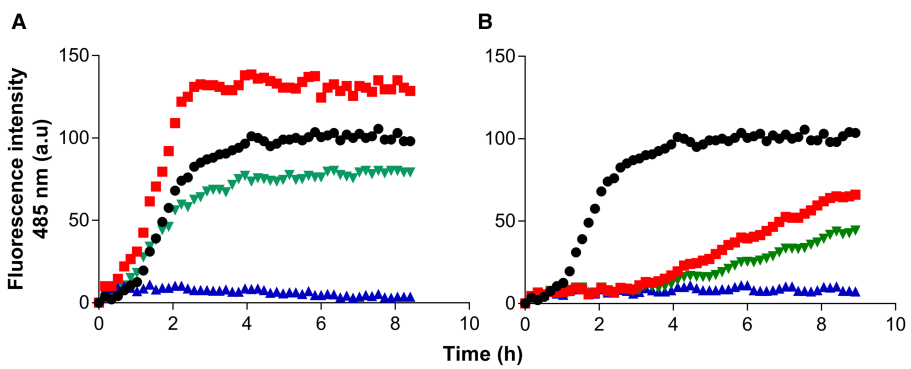

Figure 4. The inhibitory effect $A\beta42_{DM}$ has on the aggregation kinetics of seeded Aβ42.

ThT fluorescence was monitored upon incubation of Aβ42 (4 μM), $A\beta42_{DM}$ (62 nM) or co-incubation of both peptides with 400 nM Aβ42 seeds at 37°C with continuous shaking (**A**) or 400 nM of seeds from inhibited reaction (a mixture of $A\beta42_{DM}$ and Aβ42 at a 1:65 molar ratio) (**B**) black — Aβ42; red — Aβ42 with seeds; blue — $A\beta42_{DM}$ with seeds; green — Aβ42 and $A\beta42_{DM}$ with seeds. The initial values from each sample were subtracted.

Biochemical Journal (2018) **475** 3087–3103
https://doi.org/10.1042/BCJ20180247

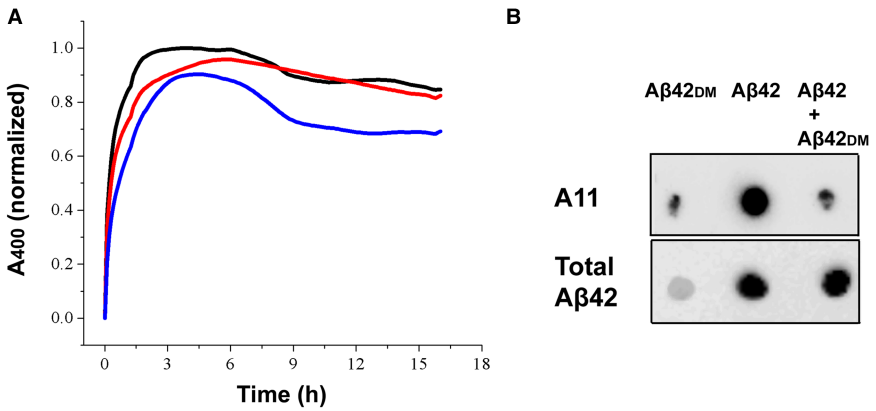

Figure 5. Aβ42$_{DM}$ modulates the Aβ42 aggregation pathway.

(**A**) Light scattering was monitored at 400 nm over the course of Aβ42 aggregation in the presence of Aβ42$_{DM}$. Black, red, and blue lines represent samples of Aβ42 (4 μM), Aβ42, and Aβ42$_{DM}$ at 1:65 molar ratios (Aβ42$_{DM}$:Aβ42) and Aβ42$_{DM}$ (62 nM), respectively. (**B**) A dot blot analysis. Aβ42 (4 μM) incubated for 18 h in the presence or absence of Aβ42$_{DM}$ (62 nM) was assessed in a dot blot experiment using anti-A11 antibodies. The total amount of Aβ42 was detected by blotting with anti-Aβ42 antibodies.

to that seen in HEK293T cells (Figure 6C). Importantly, upon monitoring cell toxicity in HEK-Aβ42-GFP-Aβ42$_{DM}$L and HEK-Aβ42-GFP-Aβ42$_{DM}$H cells, as opposed to HEK-Aβ42-GFP cells, where no inhibitory effect was observed, we found that Aβ42-induced toxicity was reduced in a manner dependent on Aβ42$_{DM}$ expression levels, being completely abolished in the presence of high Aβ42$_{DM}$ expression (Figure 6A). This implies that Aβ42$_{DM}$ is highly efficient as an Aβ42 inhibitor, blocking Aβ42-mediated aggregation and cell toxicity.

In addition to intracellular Aβ42 toxicity, Aβ42 extracellular fibrils and aggregates are also known to induce neuronal cell death [44]. Therefore, we tested the ability of Aβ42$_{DM}$ to inhibit Aβ42-mediated toxicity upon incubation with extracellular aggregates in SH-SY5Y cells incubated with Aβ42 fibrils in the presence or absence of Aβ42$_{DM}$ peptide, with cell viability being monitored by the XTT assay. The assay was performed at 1:571, 1:266, and 1:65 molar ratios of Aβ42$_{DM}$ and Aβ42 (2 μM of Aβ42 and 7, 15, or 31 nM of Aβ42$_{DM}$, respectively; Figure 6B). Our results demonstrated that Aβ42 fibrils that were pre-formed extracellularly (as confirmed by ThT and TEM, Figure 3A,B, respectively), reduced cell viability by ∼40–50%, relative to control SH-SY5Y cells that had not been treated with aggregated Aβ42 fibrils. Not surprisingly, 32 nM Aβ42$_{DM}$ alone (the highest concentration tested) had only minor effects on cell viability (∼10% reduction). Importantly, in SH-SY5Y cells introduced to Aβ42 that had been allowed to aggregate in the presence of different concentrations of Aβ42$_{DM}$, Aβ42-mediated toxicity was significantly reduced in a dose-dependent manner, and exhibited ∼90% of the viability of naïve cells (Figure 6B).

Having demonstrated that Aβ42$_{DM}$ can prevent Aβ42-mediated toxicity when the two were co-expressed in the cell or when added externally together following Aβ42 aggregation (Figure 6A,B), we tested whether the external addition of Aβ42$_{DM}$ could prevent the intracellular Aβ42-mediated toxicity in neuronal SH-SY5Y cells stably expressing Aβ42, and whether neuronal cells stably expressing Aβ42$_{DM}$ were less affected by the external addition of Aβ42 fibrils. For this, we generated SH-SY5Y cells stably expressing Aβ42-GFP (designated SH-Aβ42-GFP) or Aβ42$_{DM}$-GFP (designated SH-Aβ42$_{DM}$-GFP), as confirmed by WB analysis (Supplementary Figure S8F). An XTT cell viability assay was performed with SH-Aβ42-GFP cells incubated in the presence of extracellular Aβ42$_{DM}$ peptide at different concentrations (10–500 nM; Figure 6C). Our results indicated that SH-Aβ42-GFP cells were ∼35–40% less viable, relative to naïve SH-SY5Y cells, or to naïve SH-SY5Y cells treated with externally added Aβ42$_{DM}$ (500 nM). However, upon the addition of Aβ42$_{DM}$ to SH-Aβ42-GFP cells at concentrations of 10, 50, or 500 nM, Aβ42-GFP-mediated cell toxicity was significantly reduced in a dose-dependent manner (Figure 6C). In particular, when treated with 500 nM Aβ42$_{DM}$, SH-Aβ42-GFP cells exhibited increased viability up to 91%, relative to control cells (naïve SH-SY5Y cells) (Figure 6C).

Biochemical Journal (2018) 475 3087–3103
https://doi.org/10.1042/BCJ20180247

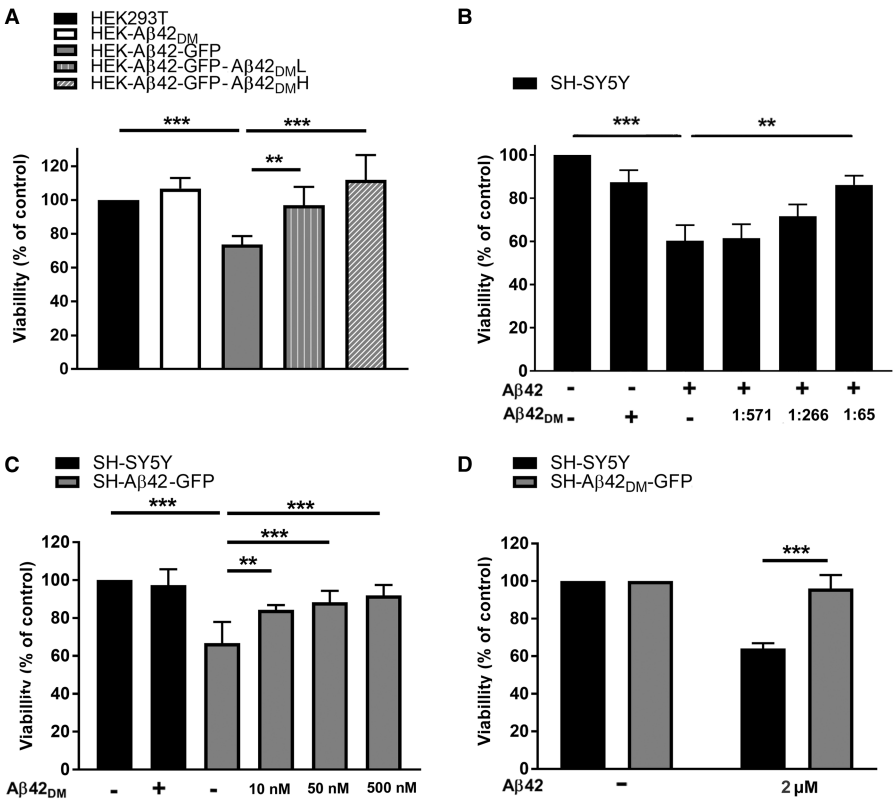

Figure 6. Aβ42$_{DM}$ reduces Aβ42 toxicity in cells.

(**A**) HEK293T cells stably expressing Aβ42-GFP (dark gray), Aβ42$_{DM}$ (white), or a combination of the two proteins, with low Aβ42$_{DM}$ expression ($_{DM}$L, dark gray with vertical white stripes) or high Aβ42$_{DM}$ expression ($_{DM}$H, dark gray with diagonal white stripes), as analyzed by FACS based on GFP and BFP fluorescence (as shown in Supplementary Figure S7A–E), were subjected to an XTT cell viability assay. (**B**) SH-SY5Y cells were introduced to 2 μM extracellular Aβ42 fibrils with or without Aβ42$_{DM}$ at different molar ratios (Aβ42$_{DM}$:Aβ42), as indicated in the graph. After 24 h, the cells were subjected to XTT cell viability assay. (**C**) SH-SY5Y cells stably expressing Aβ42-GFP (dark gray) were incubated with 10–500 nM of Aβ42$_{DM}$. After 24 h, the cells were subjected to a XTT cell viability assay. Protein expression was confirmed by WB analysis (Supplementary Figure S4B). (**D**) SH-SY5Y cells (black) and SH-SY5Y cells that stably expressed Aβ42$_{DM}$ (dark gray) were incubated with 2 μM Aβ42 fibrils. After 24 h, the cells were subjected to a XTT cell viability assay. Protein expression was confirmed by WB analysis (Supplementary Figure S4B). Quantitative analysis ($n = 3$) was performed by unpaired Student's *t*-test. **, $P < 0.05$; ***, $P < 0.005$. Error bars indicate the standard error of independent experiments performed in triplicate.

We next monitored the viability of SH-Aβ42$_{DM}$-GFP cells incubated with 2 μM extracellular purified Aβ42 fibrils (Figure 6D). Our results show that upon extracellular addition of 2 μM Aβ42 peptide, the viability of naïve SH-SY5Y cells was reduced by ∼40–50%. SH-Aβ42$_{DM}$-GFP cells were, however, resistant to the toxic effects of Aβ42 and their viability was similar to that of non-treated SH-Aβ42$_{DM}$-GFP cells (∼5% reduction).

In relation to the diffuse non-aggregating expression pattern of Aβ42$_{DM}$ seen in cells (Figure 1D), the results presented in Figure 6A–D indicated that the non-aggregating variants of Aβ42, such as Aβ42$_{DM}$, had a lower toxic effect in the cells, when compared with Aβ42. These results further confirm that protein aggregation plays a major role in induced neuronal cell death.

Aβ42$_{DM}$ peptide prevents Aβ42 uptake by cells

Given our demonstration that Aβ42$_{DM}$ significantly reduced the toxicity of intracellular and extracellular Aβ42 in both neuronal and non-neuronal cells (Figure 6), we looked to further elucidate the mechanism of the inhibitory effect. As re-uptake of extracellular Aβ42 protein aggregates is considered to be a key determinant for Aβ42-induced neuronal cell death [45], we next analyzed whether Aβ42$_{DM}$ had an effect on Aβ42 uptake

Biochemical Journal (2018) **475** 3087–3103
https://doi.org/10.1042/BCJ20180247

by cells. For this, we used Hilyte-488-labeled Aβ42 peptide (designated Aβ42-488), which was allowed to extracellularly aggregate and form fibrils in the absence or presence of $Aβ42_{DM}$ at a molar ratio of 1:65 ($Aβ42_{DM}$:Aβ42-488) before being introduced into SH-SY5Y neuronal cells. Aβ42-488 entry into and localization within cells was monitored by confocal microscopy (Figure 7). Our results showed that 18 h post-incubation, the Aβ42-488 peptide had formed aggregates and was localized as inclusion bodies inside the cells (Figure 7). However, when Aβ42-488 was incubated with $Aβ42_{DM}$, most of the labeled peptide was localized on the cell membrane and fewer aggregates were seen, suggesting that the labeled peptide could not enter the cell (Figure 7). Quantifying the accumulation of Aβ42-488 within the cells using the Operetta high-content imaging system showed a decrease in ∼50% in Aβ42-488 entry into cells in the presence of $Aβ42_{DM}$ (Supplementary Figure S9). We conclude that $Aβ42_{DM}$ prevents Aβ42 uptake by the cells, providing a possible explanation for the Aβ42-mediated inhibition of cell toxicity observed in Figure 6B.

Discussion

In the present study, we investigated the potential of $Aβ42_{F19S,L34P}$ ($Aβ42_{DM}$), an Aβ42 variant carrying two mutations, as an inhibitor of Aβ42 aggregation. We showed that $Aβ42_{DM}$ suppressed Aβ42 aggregation *in vitro* and modulated its aggregation pathway into non-toxic off-pathway aggregates, as well as intracellular Aβ42 aggregation, and reduced Aβ42-mediated cell toxicity in neuronal and non-neuronal cells. We also demonstrated that $Aβ42_{DM}$ prevented internalization of pre-formed Aβ42 aggregates, providing a mechanistic explanation for its inhibitory effects.

$Aβ42_{DM}$ was previously characterized as a non-aggregating mutant of Aβ42 that cannot self-assemble within the cell when expressed in bacteria or in mammalian cells [30,39]. We were thus interested in testing whether $Aβ42_{DM}$ still binds Aβ42 and prevents Aβ42 aggregation by acting as a dominant-negative inhibitor with antagonistic activity. This assumption was based on a recent study highlighting the potential of the Aβ42 variant $Aβ42_{G37L}$ to efficiently inhibit Aβ42 aggregation and the toxicity that follows [46]. Accordingly, we examined the ability of $Aβ42_{DM}$ to efficiently inhibit Aβ42 aggregation both *in vitro* and in a variety of cell model-based assays that mimic and address both the intracellular and extracellular aggregation of Aβ42 and further examined the effects of $Aβ42_{DM}$ on both intracellular and extracellular aggregated Aβ42-mediated cell toxicity.

It has been previously shown that the self-assembly of Aβ42 is crucial for its cellularly mediated toxic effects. A recent study showed that an Aβ42 variant ($Aβ42_{F19S,G37D}$) that is incapable of self-assembly and oligomerization is non-toxic to cells [35]. This observation is with agreement with our results which also show that $Aβ42_{DM}$ lacks the ability to aggregate in cells (Figure 1) or *in vitro* (Supplementary Figure S4) and is also non-toxic to cells (Figure 6). Importantly, by disturbing Aβ42 aggregation (Figures 1 and 3), $Aβ42_{DM}$ also significantly reduced both intracellular and extracellular Aβ42-mediated toxicity (Figure 6).

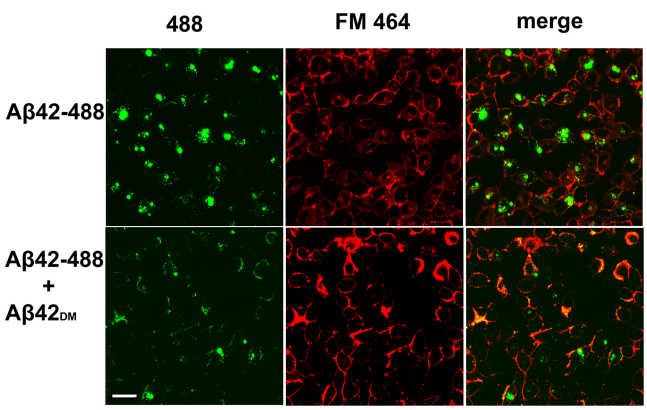

Figure 7. $Aβ42_{DM}$ prevents Aβ42 penetration into cells.

SH-SY5Y cells were incubated with 500 nM Aβ42-Hilyte 488-labeled aggregates in the presence or absence of 7.75 nM $Aβ42_{DM}$ for 18 h. FM-4-64 dye was used to stain the cell membrane. Live imaging was performed using an Olympus confocal microscope. The scale bar indicates 150 μm.

Biochemical Journal (2018) 475 3087–3103
https://doi.org/10.1042/BCJ20180247

The classical amyloid cascade hypothesis suggests that extracellular amyloid plaques are the main driving force in AD pathogenesis [44,47]. However, more recent data also highlight the crucial role of intracellular Aβ42 accumulation and aggregation [9,11,45,48]. Our results show that intracellular Aβ42 is toxic to cells and reduces both neuronal and non-neuronal cell viability (Figure 6). As it is challenging to model the toxic effects of Aβ42 in cell culture, we believe that it is important to develop cell-based assays to better understand the pathogenic mechanism of Aβ42 at the cellular level.

To provide a mechanistic explanation for the effects of $Aβ42_{DM}$ and to elucidate whether $Aβ42_{DM}$ suppresses intracellular and extracellular Aβ42 aggregation through direct binding, we tested whether direct interactions between $Aβ42_{DM}$ and Aβ42 exist by SPR (Figure 2B,C). We found that $Aβ42_{DM}$ does not bind monomeric Aβ42 (Figure 2C), yet it does bind oligomeric Aβ42 (Figure 2B). We further analyzed $Aβ42_{DM}$ activity against Aβ42 aggregation by *in vitro* ThT staining, TEM, and assessing oligomerization levels (Figure 3). As we showed that $Aβ42_{DM}$ suppressed Aβ42 aggregation, we aimed to better understand the mechanism of $Aβ42_{DM}$-mediated inhibition. We showed that $Aβ42_{DM}$ allowed the formation of Aβ42 oligomers, as revealed by light scattering (Figure 5A); however, these oligomers were significantly less well-recognized by the A11 antibody, which recognizes toxic 'on-pathway' Aβ oligomers [42,43]. Moreover, in contrast with Aβ42 aggregates that induce monomeric Aβ42 aggregation and shorten the lag phase when added as seeds to the Aβ42 monomers (Figure 4A), Aβ42 aggregates formed in the presence of $Aβ42_{DM}$ did not induce aggregation of the monomers or shorten the lag phase, and surprisingly, acted as potent inhibitors, reducing the Aβ42 monomer aggregation and extending the lag phase (Figure 4B). Finally, aggregates formed in the presence of $Aβ42_{DM}$ suppressed toxicity in a dose-dependent manner, in comparison with untreated Aβ42 aggregates (Figure 6B). As we also showed by ThT that $Aβ42_{DM}$ does not affect Aβ42 aggregation when added after 24 h (Supplementary Figure S6), we conclude that $Aβ42_{DM}$ interacts with low molecular-weight oligomers but not with either high molecular-weight (or prefibrillar) oligomers or monomers of Aβ42 and thus directs these low molecular-weight oligomers into 'off-pathway' non-toxic aggregates.

In fact, these features above make $Aβ42_{DM}$ different from other Aβ peptides, such as Aβ40, for example. Although sharing high sequence similarity with Aβ42 and $Aβ42_{DM}$, Aβ40 can act as both an inhibitor and an inducer of Aβ42 aggregation [41,50–52]. Specifically, Aβ40 inhibits the aggregation of Aβ42 monomers in a concentration-dependent manner [50–52]. On the other hand, it has been shown that cross-seeding of Aβ40 fibrils and Aβ42 monomers promotes Aβ42 aggregation [41]. The cross-seeding effects of Aβ40 and Aβ42 probably result from the sequence similarity and structural plasticity of the two proteins, allowing Aβ42 monomers to adopt the fibril structure of Aβ40 seeds and promoting Aβ42 aggregation in the presence of these seeds [41]. In contrast with Aβ40 seeds that induce Aβ42 aggregation, the seeds formed in the presence of $Aβ42_{DM}$ did not induce Aβ42 aggregation but instead acted as a potent inhibitor. This difference in mode of action of Aβ40 and $Aβ42_{DM}$ is probably a result of the two $Aβ42_{DM}$ mutations at positions 19 and 34 (both lie within the β-sheet hydrophobic/aggregation-prone regions 17–20 and 31–36 [49] of Aβ42), which do not allow fibril formation [30]. In contrast, these two regions are intact and have wild-type sequences in Aβ40.

Our results show that the binding affinity between $Aβ42_{DM}$ and Aβ42 is relatively low (K_D = 520 nM), as compared with those of other inhibitors. For example, a recent study describing new inhibitors of Aβ42-mediated aggregation showed that several Anticalins, which are based on the human lipocalin affinity scaffold and were screened against Aβ40, displayed binding affinities to Aβ40 and Aβ42 of less than 100 pM [53]. However, for these inhibitors to be efficient in inhibiting amyloid aggregation and reducing cell toxicity, a 1:1 molar ratio of the inhibitor and its target, Aβ40, was required. In contrast, $Aβ42_{DM}$ is effective in reducing Aβ42 fibril formation *in vitro*, even at a molar ratio of 1:266 ($Aβ42_{DM}$:Aβ42).

Considering the binding kinetics of Aβ42 to $Aβ42_{DM}$ and the inhibition efficiency of Aβ42 aggregation by $Aβ42_{DM}$, i.e. low binding affinity of $Aβ42_{DM}$ to Aβ42 (K_D of 520 nM) and high inhibition efficiency for $Aβ42_{DM}$ against Aβ42, we predict that $Aβ42_{DM}$ rapidly associates with and dissociates from Aβ42 (with k_{on} and k_{off} rates of 300 M^{-1} s^{-1} and 1.6 × 10^{-4} s^{-1}, respectively), such that each $Aβ42_{DM}$ molecule potentially binds to and dissociates from multiple Aβ42 oligomers in a sequential manner, thereby disturbing and modulating oligomer self-assembly. Consequently, the very low molar ratio of 1:266-1:65 (as seen in Figure 3) is sufficient to suppress Aβ42 aggregation and to reduce Aβ42 toxicity, as seen in Figure 6B. Since other inhibitors with higher binding affinity, such as the anticalins noted above [53], require higher molar ratios (in favor of the inhibitor) to bind and efficiently inhibit their targets, $Aβ42_{DM}$ offers a major advantage in terms of activity efficiency and potential therapeutic advantage, as the low doses required result in reduced toxicity and side effects.

Finally, re-uptake of extracellular aggregates into neuronal cells is thought to be a key factor in inducing neuronal cell death [45]. As such, we explored whether $A\beta42_{DM}$ affects Aβ42 uptake and internalization by cells to better understand the inhibition of extracellular Aβ42-mediated cell toxicity by soluble $A\beta42_{DM}$, as shown in Figure 6B. Aβ42 interacts with several different transporters on the membrane that permit entry into neuronal cells [10,54–56]. Our results show that labeled Aβ42 peptide (Aβ42-488) entered SH-SY5Y neuronal cells after 18 h of incubation with the cells (Figure 7). However, the presence of $A\beta42_{DM}$ in a molar ratio of 1:65 ($A\beta42_{DM}$:Aβ42-488) significantly prevented Aβ42-488 internalization (Figure 7). This result matches our data demonstrating that external addition of synthetic Aβ42 caused a toxic effect that was abolished upon expression of $A\beta42_{DM}$ or upon addition of $A\beta42_{DM}$ to the medium as soluble protein (Figure 6B,D).

These results provide a possible explanation for the inhibition of Aβ42-mediated toxicity, namely as the result of Aβ42 uptake and internalization into cells, where it induces toxic effects and cell death. The presence of $A\beta42_{DM}$ not only disturbed the aggregation process and modulated the aggregation pathway but also prevented Aβ42 internalization and thus protected cells from Aβ42-mediated toxicity. Considering our results showing the protective activity of $A\beta42_{DM}$ against intracellular and extracellular Aβ42 when expressed in cells or added externally as soluble protein, it would appear that $A\beta42_{DM}$ has the potential to be used therapeutically as soluble protein or as intracellularly expressed protein.

In summary, our results highlight the efficient activity of $A\beta42_{DM}$ against both intracellular and extracellular aggregation of Aβ42. In the past, many inhibitors were designed to disrupt Aβ42 aggregation; however, most were addressed solely in terms of their ability to prevent extracellular aggregation [57,58], although some were addressed in terms of their ability to prevent intracellular aggregation [28,39]. Still, there is a lack of knowledge on inhibitors which target both intracellular and extracellular aggregates. As emerging evidence suggests that both intracellular and extracellular aggregation induces neuronal cell death, it is important to develop inhibitors able to inhibit both the intra- and extracellular aggregation, such as $A\beta42_{DM}$. We thus suggest further exploration of $A\beta42_{DM}$ as a novel AD therapeutic.

Abbreviations

AD, Alzheimer's disease; APP, amyloid precursor protein; Aβ, amyloid β; CD, circular dichroism; ECM, extracellular matrix; FBS, fetal bovine serum; HRP, horseradish peroxidase; IP, immunoprecipitation; IRES, internal ribosome entry site; PBS, phosphate-buffered saline; PI, protease inhibitor; RU, response unit; SPR, surface plasmon resonance; TEM, transmission electron microscope; ThT, thioflavin T; WB, western blot.

Author Contribution

O.O., R.T., and N.P. designed the research; O.O. and V.B. performed the research; O.O., R.T., and N.P. analyzed the data; O.O., R.T., and N.P. wrote the paper. All authors edited the manuscript and approved the final version.

Funding

This work was supported by the US-Israel Binational Science Foundation [contract grant number: 2015134] to N.P. R.T. acknowledges support from the Israel Science Foundation [contract grant number: 755/17].

Acknowledgments

The authors thank Ravit Malishev, Prof. Raz Jelinek, Shiran Lacham, Bar Dagan, Dr Alon Zilka, and Dr Uzi Hadad for their technical assistance. FACS experiments were performed at the Ilse Katz Institute for Nanoscale Science and Technology, BGU. Confocal microscopy experiments were performed at the NIBN proteomics unit, BGU.

Competing Interests

The Authors declare that there are no competing interests associated with the manuscript.

References

1 Wu, Y.-T., Beiser, A.S., Breteler, B., Fratiglioni, M.M., Helmer, L., Hendrie, C., et al. (2017) The changing prevalence and incidence of dementia over time — current evidence. *Nat. Rev. Neurol.* **13**, 327–339 https://doi.org/10.1038/nrneurol.2017.63
2 Nussbaum, J.M., Seward, M.E. and Bloom, G.S. (2013) Alzheimer disease: a tale of two prions. *Prion* **7**, 14–19 https://doi.org/10.4161/pri.22118
3 Haass, C. and Selkoe, D.J. (2007) Soluble protein oligomers in neurodegeneration: lessons from the Alzheimer's amyloid β-peptide. *Nat. Rev. Mol. Cell Biol.* **8**, 101–112 https://doi.org/10.1038/nrm2101
4 Selkoe, D.J. (2003) Folding proteins in fatal ways. *Nature* **426**, 900–904 https://doi.org/10.1038/nature02264

Biochemical Journal (2018) **475** 3087–3103
https://doi.org/10.1042/BCJ20180247

5 McNaull, B.B.A., Todd, S., McGuinness, B. and Passmore, A.P. (2010) Inflammation and anti-inflammatory strategies for Alzheimer's disease — a mini-review. *Gerontology* **56**, 3–14 https://doi.org/10.1159/000237873

6 Lucas, S.-M., Rothwell, N.J. and Gibson, R.M. (2006) The role of inflammation in CNS injury and disease. *Br. J. Pharmacol.* **147**, S232–S240 https://doi.org/10.1038/sj.bjp.0706400

7 Rojo, L.E., Fernández, J.A., Maccioni, A.A., Jimenez, J.M. and Maccioni, R.B. (2008) Neuroinflammation: implications for the pathogenesis and molecular diagnosis of Alzheimer's disease. *Arch. Med. Res.* **39**, 1–16 https://doi.org/10.1016/j.arcmed.2007.10.001

8 Lee, S.J.C., Nam, E., Lee, H.J., Savelieff, M.G. and Lim, M.H. (2017) Towards an understanding of amyloid-β oligomers: characterization, toxicity mechanisms, and inhibitors. *Chem. Soc. Rev.* **46**, 310–323 https://doi.org/10.1039/C6CS00731G

9 LaFerla, F.M., Green, K.N. and Oddo, S. (2007) Intracellular amyloid-β in Alzheimer's disease. *Nat. Rev. Neurosci.* **8**, 499–509 https://doi.org/10.1038/nrn2168

10 Wilson, C.A., Doms, R.W. and Lee, V.M.-Y. (1999) Intracellular APP processing and AB production in Alzheimer disease. *J. Neurophatol. Exp. Neurol.* **58**, 787–794 PMID:10446803

11 Umeda, T., Tomiyama, T., Sakama, N., Tanaka, S., Lambert, M.P., Klein, W.L. et al. (2011) Intraneuronal amyloid β oligomers cause cell death via endoplasmic reticulum stress, endosomal/lysosomal leakage, and mitochondrial dysfunction in vivo. *J. Neurosci. Res.* **89**, 1031–1042 https://doi.org/10.1002/jnr.22640

12 Cho, D.-H., Nakamura, T., Fang, J., Cieplak, P., Godzik, A., Gu, Z. et al. (2009) S-nitrosylation of Drp1 mediates β-amyloid-related mitochondrial fission and neuronal injury. *Science* **324**, 102–105 https://doi.org/10.1126/science.1171091

13 Resende, R., Ferreiro, E., Pereira, C. and Resende de Oliveira, C. (2008) Neurotoxic effect of oligomeric and fibrillar species of amyloid-beta peptide 1-42: involvement of endoplasmic reticulum calcium release in oligomer-induced cell death. *Neuroscience* **155**, 725–737 https://doi.org/10.1016/j.neuroscience.2008.06.036

14 Caspersen, C., Wang, N., Yao, J., Sosunov, A., Chen, X., Lustbader, J.W. et al. (2005) Mitochondrial Aβ: a potential focal point for neuronal metabolic dysfunction in Alzheimer's disease. *FASEB J.* **19**, 2040–2041 https://doi.org/10.1096/fj.05-3735fje

15 Hoozemans, J.J.M., Veerhuis, R., Van Haastert, E.S., Rozemuller, J.M., Baas, F., Eikelenboom, P. et al. (2005) The unfolded protein response is activated in Alzheimer's disease. *Acta Neuropathol.* **110**, 165–172 https://doi.org/10.1007/s00401-005-1038-0

16 Keil, U., Bonert, A., Marques, C.A., Scherping, I., Weyermann, J., Strosznajder, J.B. et al. (2004) Amyloid β-induced changes in nitric oxide production and mitochondrial activity lead to apoptosis. *J. Biol. Chem.* **279**, 50310–50320 https://doi.org/10.1074/jbc.M405600200

17 Tjernberg, L.O., Lilliehöök, C., Callaway, D.J., Näslund, J., Hahne, S., Thyberg, J. et al. (1997) Controlling amyloid β-peptide fibril formation with protease-stable ligands. *J. Biol. Chem.* **272**, 12601–12605 https://doi.org/10.1074/jbc.272.19.12601

18 Tjernberg, L.O., Näslund, J., Lindqvist, F., Johansson, J., Karlström, A.R., Thyberg, J. et al. (1996) Arrest of beta-amyloid fibril formation by a pentapeptide ligand. *J. Biol. Chem.* **271**, 8545–8548 https://doi.org/10.1074/jbc.271.15.8545

19 Neddenriep, B. (2011) Short peptides as inhibitors of amyloid aggregation. *Open Biotechnol. J.* **5**, 39–46 https://doi.org/10.2174/1874070701105010039

20 Lin, L.X., Bo, X.Y., Tan, Y.Z., Sun, F.X., Song, M., Zhao, J. et al. (2014) Feasibility of β-sheet breaker peptide-H102 treatment for Alzheimer's disease based on β-Amyloid hypothesis. *PLoS ONE* **9**, e112052 https://doi.org/10.1371/journal.pone.0112052

21 Taylor, M., Moore, S., Mayes, J., Parkin, E., Beeg, M., Canovi, M. et al. (2010) Development of a proteolytically stable retro-inverso peptide inhibitor of β-amyloid oligomerization as a potential novel treatment for Alzheimer's disease. *Biochemistry* **49**, 3261–3272 https://doi.org/10.1021/bi100144m

22 Bett, C.K., Serem, W.K., Fontenot, K.R., Hammer, R.P. and Garno, J.C. (2010) Effects of peptides derived from terminal modifications of the AB central hydrophobic core on AB fibrillization. *ACS Chem. Neurosci.* **1**, 661–678 https://doi.org/10.1021/cn900019r

23 Matharu, B., El-Agnaf, O., Razvi, A. and Austen, B.M. (2010) Development of retro-inverso peptides as anti-aggregation drugs for β-amyloid in Alzheimer's disease. *Peptides* **31**, 1866–1872 https://doi.org/10.1016/j.peptides.2010.06.033

24 Ghosh, A., Pradhan, N., Bera, S., Datta, A., Krishnamoorthy, J., Jana, N.R. et al. (2017) Inhibition and degradation of amyloid beta (Aβ40) fibrillation by designed small peptide: A combined spectroscopy, microscopy, and cell toxicity study. *ACS Chem. Neurosci.* **8**, 718–722 https://doi.org/10.1021/acschemneuro.6b00349

25 Young, S. and S, C. (2018) A systematic review of antiamyloidogenic and metal-chelating peptoids: two structural motifs for the treatment of Alzheimer's disease. *Molecules* **23**, 296 https://doi.org/10.3390/molecules23020296

26 Baig, M.H., Ahmad, K., Rabbani, G. and Choi, I. (2018) Use of peptides for the management of Alzheimer's disease: diagnosis and inhibition. *Front. Aging Neurosci.* **10**, 1–6 https://doi.org/10.3389/fnagi.2018.00021

27 Aileen Funke, S. and and Willbold, D. (2012) Peptides for therapy and diagnosis of Alzheimer's disease. *Curr. Pharm. Design* **18**, 755–767 https://doi.org/10.2174/138161212799277752

28 Hussein, R.M., Hashem, R.M., Rashed, L.A. and Maggio, N. (2015) Evaluation of the amyloid beta-GFP fusion protein as a model of amyloid beta peptides-mediated aggregation: a study of DNAJB6 chaperone. *Front. Mol. Neurosci.* **8**, 40–49 https://doi.org/10.3389/fnmol.2015.00040

29 Kim, W., Kim, Y., Min, J., Kim, D.J., Chang, Y.T. and Hecht, M.H. (2006) A high-throughput screen for compounds that inhibit aggregation of the Alzheimer's peptide. *ACS Chem. Biol.* **1**, 461–469 https://doi.org/10.1021/cb600135w

30 Wurth, C., Guimard, N.K. and Hecht, M.H. (2002) Mutations that reduce aggregation of the Alzheimer's Aβ42 peptide: an unbiased search for the sequence determinants of aβ amyloidogenesis. *J. Mol. Biol.* **319**, 1279–1290 https://doi.org/10.1016/S0022-2836(02)00399-6

31 Esler, W.P., Stimson, E.R., Ghilardi, J.R., Lu, Y.-A., Felix, A.M., Vinters, H.V. et al. (1996) Point substitution in the central hydrophobic cluster of a human β-amyloid congener disrupts peptide folding and abolishes plaque competence. *Biochemistry* **35**, 13914–13921 https://doi.org/10.1021/bi961302+

32 Hilbich, C., Kisters-Woike, B., Reed, J., Masters, C.L. and Beyreuther, K. (1991) Aggregation and secondary structure of synthetic amyloid βA4 peptides of Alzheimer's disease. *J. Mol. Biol.* **218**, 149–163 https://doi.org/10.1016/0022-2836(91)90881-6

33 Fay, D.S., Fluet, A., Johnson, C.J. and Link, C.D. (1998) In vivo aggregation of β-amyloid peptide variants. *J. Neurochem.* **71**, 1616–1625 https://doi.org/10.1046/j.1471-4159.1998.71041616.x

34 Pike, C.J., Walencewicz-Wasserman,, A.J., Kosmoski, J., Cribbs, D.H., Glabe, C.G. and Cotman, C.W. (1995) Structure-Activity analyses of β-Amyloid peptides: Contributions of the β25-35 region to aggregation and neurotoxicity. *J. Neurochem.* **64**, 253–265 https://doi.org/10.1046/j.1471-4159.1995.64010253.x
35 Marshall, K. E., Vadukul, D. M., Dahal, L., Theisen, A., Fowler, M. W. and Al-Hilaly, Y., *et al.* (2016) A critical role for the self-assembly of amyloid-β1-42 in neurodegeneration. *Sci. Rep.* **6**, 30182 https://doi.org/10.1038/srep30182
36 Banerjee, V., Shani, T., Katzman, B., Vyazmensky, M., Papo, N., Israelson, A. et al. (2016) Superoxide dismutase 1 (SOD1)-Derived peptide inhibits amyloid aggregation of familial amyotrophic lateral sclerosis SOD1 mutants. *ACS Chem. Neurosci.* **7**, 1595–1606 https://doi.org/10.1021/acschemneuro.6b00227
37 Banerjee, V., Oren, O., Ben-Zeev, E., Taube, R., Engel, S. and Papo, N. (2017) A computational combinatorial approach identifies a protein inhibitor of superoxide dismutase 1 misfolding, aggregation, and cytotoxicity. *J. Biol. Chem.* **292**, 15777–15788 https://doi.org/10.1074/jbc.M117.789610
38 Drescher, D.G., Drescher, M.J. and Ramakrishnan, N.A. (2009) Surface plasmon resonance (SPR) analysis of binding interactions of proteins in inner-ear sensory epithelia. *Aud. Vestibular Res.* **493**, 323–343. https://doi.org/10.1007/978-1-59745-523-7_20
39 Ochiishi, T., Doi, M., Yamasaki, K., Hirose, K., Kitamura, A., Urabe, T. et al. (2016) Development of new fusion proteins for visualizing amyloid-β oligomers in vivo. *Sci. Rep.* **6**, 22712 https://doi.org/10.1038/srep22712(2016)
40 Bieschke, J., Russ, J., Friedrich, R.P., Ehrnhoefer, D.E., Wobst, H., Neugebauer, K. et al. (2010) EGCG remodels mature α-synuclein and amyloid-β fibrils and reduces cellular toxicity. *Proc. Natl Acad. Sci. U.S.A.* **107**, 7710–7715 https://doi.org/10.1073/pnas.0910723107
41 Tran, J., Chang, D., Hsu, F., Wang, H. and Guo, Z. (2017) Cross-seeding between Aβ40 and Aβ42 in Alzheimer's disease. *FEBS Lett.* **591**, 177–185 https://doi.org/10.1002/1873-3468.12526
42 Glabe, C.G. (2008) Structural classification of toxic amyloid oligomers. *J. Biol. Chem.* **283**, 29639–29643 https://doi.org/10.1074/jbc.R800016200
43 Krishnan, R., Goodman, J.L., Mukhopadhyay, S., Pacheco, C.D., Lemke, E.A., Deniz, A.A. et al. (2012) Conserved features of intermediates in amyloid assembly determine their benign or toxic states. *Proc. Natl Acad. Sci. U.S.A.* **109**, 11172–11177 https://doi.org/10.1073/pnas.1209527109
44 Hardy, J. and Higgins, G. (1992) Alzheimer's disease: the amyloid cascade hypothesis. *Science* **256**, 184–185 https://doi.org/10.1126/science.1566067
45 Knobloch, M., Konietzko, U., Krebs, D.C. and Nitsch, R.M. (2007) Intracellular Aβ and cognitive deficits precede β-amyloid deposition in transgenic arcAβ mice. *Neurobiol. Aging* **28**, 1297–1306 https://doi.org/10.1016/j.neurobiolaging.2006.06.019
46 Adams, D.J., Nemkov, T.G., Mayer, J.P., Old, W.M. and Stowell, M.H.B. (2017) Identification of the primary peptide contaminant that inhibits fibrillation and toxicity in synthetic amyloid-β42. *PloS ONE* **12**, e0182804 https://doi.org/10.1371/journal.pone.0182804
47 Hardy, J. and Selkoe, D.J. (2002) The amyloid hypothesis of Alzheimer's disease: progress and problems on the road to therapeutics. *Science* **297**, 353–356 PMID:12130773
48 Kienlen-Campard, P., Miolet, S., Tasiaux, B. and Octave, J.N. (2002) Intracellular amyloid-β1-42, but not extracellular soluble amyloid-β peptides, induces neuronal apoptosis. *J. Biol. Chem.* **277**, 15666–15670 https://doi.org/10.1074/jbc.M200887200
49 Gu, L., Tran, J., Jiang, L. and Guo, Z. (2016) A new structural model of Alzheimer's Aβ42 fibrils based on electron paramagnetic resonance data and Rosetta modeling. *J. Struct. Biol.* **194**, 61–67 https://doi.org/10.1016/j.jsb.2016.01.013
50 Hasegawa, K., Yamaguchi, I., Omata, S., Gejyo, F. and Naiki, H. (1999) Interaction between Aβ (1- 42) and Aβ (1- 40) in Alzheimer's β-amyloid fibril formation in vitro. *Biochemistry* **38**, 15514–15521 https://doi.org/10.1021/bi991161m
51 Yan, Y. and Wang, C. (2007) Aβ40 protects non-toxic Aβ42 monomer from aggregation. *J. Mol. Biol.* **369**, 909–916 https://doi.org/10.1016/j.jmb.2007.04.014
52 Jan, A., Gokce, O., Luthi-Carter, R. and Lashuel, H.A. (2008) The ratio of monomeric to aggregated forms of Aβ40 and Aβ42 is an important determinant of amyloid-β aggregation, fibrillogenesis, and toxicity. *J. Biol. Chem.* **283**, 28176–28189 https://doi.org/10.1074/jbc.M803159200
53 Rauth, S., Hinz, D., Borger, M., Uhrig, M., Mayhaus, M., Riemenschneider, M. et al. (2016) High-affinity anticalins with aggregation-blocking activity directed against the Alzheimer β-amyloid peptide. *Biochem. J.* **473**, 1563–1578 https://doi.org/10.1042/BCJ20160114
54 Bu, G., Cam, J. and Zerbinatti, C. (2006) LRP in amyloid-β production and metabolism. *Ann. N. Y. Acad. Sci.* **1086**, 35–53 https://doi.org/10.1196/annals.1377.005
55 Deane, R., Du Yan, S., Submamaryan, R.K., LaRue, B., Jovanovic, S., Hogg, E. et al. (2003) RAGE mediates amyloid-β peptide transport across the blood-brain barrier and accumulation in brain. *Nat. Med.* **9**, 907–913 https://doi.org/10.1038/nm890
56 Nagele, R., D'andrea, M., Anderson, W. and Wang, H.-Y. (2002) Intracellular accumulation of β-amyloid1-42 in neurons is facilitated by the α7 nicotinic acetylcholine receptor in Alzheimer's disease. *Neuroscience* **110**, 199–211 https://doi.org/10.1016/S0306-4522(01)00460-2
57 Kuruva, C.S. and Reddy, P.H. (2017) Amyloid beta modulators and neuroprotection in Alzheimer's disease: a critical appraisal. *Drug Discovery Today* **22**, 223–233 https://doi.org/10.1016/j.drudis.2016.10.010
58 Doig, A.J. and Derreumaux, P. (2015) Inhibition of protein aggregation and amyloid formation by small molecules. *Curr. Opin. Struct. Biol.* **30**, 50–56 https://doi.org/10.1016/j.sbi.2014.12.004